

# Robust algorithms for limit load and shear strength reduction methods

Stanislav Sysala

Institute of Geonics of the Czech Academy of Sciences, Ostrava, Czech Republic

stanislav.sysala@ugn.cas.cz

December 20, 2023

## Abstract

This paper is focused on continuation techniques and Newton-like methods suggested for numerical determination of safety factors within stability assessment. Especially, we are interested in the stability of slopes and related limit load and shear strength reduction methods. We build on computational plasticity and the finite element method, but we mainly work on an algebraic level to be the topic understandable for broader class of scientists and our algorithms more transparent. The presented algorithms are based on the associated plasticity to be more robust. For non-associated models, we use Davis-type approximations enabling us to apply the associated approach. A particular attention is devoted to the Mohr-Coulomb elastic-perfectly plastic constitutive problem. On this example, we explain some important features of the presented methods which are beyond the algebraic settings of the problems. We also summarize the Mohr-Coulomb constitutive solution and some implementation details.

**Keywords:** stability assessment, safety factors, computational plasticity, finite element method, Newton-like methods, continuation techniques

## 1 Introduction

This paper is organized as follows. In Section 2, we introduce an algebraic system of nonlinear equations, relate it with a simplified elasto-plastic problem and specify assumptions typical for associative models with bounded hardening or without hardening (perfect plasticity). Section 3 is devoted to the determination of the limit load by an appropriate continuation technique and a Newton-like method. The so-called limit analysis problem is derived using the suggested continuation method. In Section 4, we explain an idea of the shear strength reduction method (SSRM) within the algebraic setting. Further, we relate SSRM with the limit load and propose a solution scheme based on an iterative limit load approach. We also show that there exists a counterpart of the limit analysis

problem for SSRM. We use it to introduce an alternative solution scheme based on a regularization method. In Section 5, we introduce the elastic-perfectly plastic model with the Mohr-Coulomb yield criterion to define SSRM more precisely, explain Davis' approximations and other features of the elasto-plastic problems which are beyond the algebraic level. We also recapitulate the constitutive solution for the investigated problem. Section 6 contains notes to the efficient implementation of the suggested algorithms in Matlab.

## 2 Algebraic system of nonlinear equations related to associated elasto-plasticity

Elasto-plastic problems after time and space discretization are often defined in terms of displacements and have the following scheme:

$$\text{find } u^* \in V_h : \int_{\Omega} T(\varepsilon(u^*)) : \varepsilon(u) dx = b(u) \quad \forall u \in V_h, \quad (2.1)$$

where  $V_h \subset \{u \in H^1(\Omega; \mathbb{R}^3) \mid u = 0 \text{ on } \Gamma_D\}$  is a finite-dimensional space of admissible displacements arising from a finite element approximation of the Sobolev space  $H^1(\Omega; \mathbb{R}^3)$ ,  $\varepsilon(u) = \frac{1}{2}(\nabla u + (\nabla u)^T)$  is the small strain tensor,  $T$  is a nonlinear constitutive operator representing a stress-strain relationship and  $b$  is a linear functional of external forces. It is worth mentioning that the operator  $T$  may depend on: plastic strain and hardening from a previous time step; the initial stress; pore pressure, etc.

The problem (2.1) can be standardly rewritten as the following algebraic system of nonlinear equations in  $\mathbb{R}^n$ :

$$\text{find } u^* \in \mathbb{R}^n : F(u^*) = b, \quad F: \mathbb{R}^n \rightarrow \mathbb{R}^n, b \in \mathbb{R}^n. \quad (2.2)$$

Now, we introduce three assumptions  $(\mathcal{A}_1)$ ,  $(\mathcal{A}_2)$  and  $(\mathcal{A}_3)$  on  $F$  which are expected for the associated elasto-plastic model with bounded hardening or without hardening:

$(\mathcal{A}_1)$   $F$  is Lipschitz continuous in  $\mathbb{R}^n$ .

This first assumption implies that  $F$  is almost everywhere differentiable in  $\mathbb{R}^n$  and that there exists a generalized derivative  $F^o: \mathbb{R}^n \rightarrow \mathbb{R}^{n \times n}$  such that  $F^o(u) = F'(u)$  if  $F$  is differentiable at  $u$ . Otherwise, it is required to be satisfied  $F^o(u) \in \partial F(u)$ , where  $\partial F(u)$  is the subdifferential of  $F$  at  $u$  in Clarke's sense. It is important to note that the elasto-plastic functions  $F$  or  $T$  are not smooth at least on the interface between the elastic and plastic branches. For sufficiently small  $u$ , one can expect that  $F^o(u) = K_{el}$  where  $K_{el}$  is the elastic stiffness matrix.

$(\mathcal{A}_2)$   $F$  is strongly semismooth in  $\mathbb{R}^n$ . In particular, we will assume that

$$\begin{aligned} \forall u \in \mathbb{R}^n, \exists L_u, \epsilon_u > 0 : \quad & \|F(v) - F(u) - F^o(v)(v - u)\| \leq L_u \|u - v\|^2 \quad \forall v \in B(u; \epsilon_u), \\ F(v) - F(u) = \int_0^1 & F^o(u + \theta(v - u))(v - u) d\theta \quad \forall u, v \in \mathbb{R}^n. \end{aligned}$$

The strong semismoothness is a crucial assumption which enables us to study local quadratic convergence of *the semismooth Newton method*:

$$u^{k+1} = u^k + [F^o(u^k)]^{-1}(b - F(u^k)), \quad k = 0, 1, \dots, \quad u^0 - \text{ given.}$$

To verify that  $F$  (or  $T$ ) is strongly semismooth, we use the following framework:

- Continuous piecewise linear functions are strongly semismooth with  $L_u = 0$ .
- Smooth functions with locally Lipschitz continuous derivatives are strongly semismooth.
- Finite sums, products or compositions of semismooth functions are again semismooth.
- There exists the implicit function theorem for semismooth functions, see [17].

Let us note that the elasto-plastic operators are often implicit if the implicit Euler method is used for time discretization. Further, the assumptions  $(\mathcal{A}_1)$  and  $(\mathcal{A}_2)$  are expected also in non-associated plasticity unlike the following assumption.

$(\mathcal{A}_3)$   $F$  has a convex potential in  $\mathbb{R}^n$  with at least linear growth at infinity, i.e.,

- $\exists \mathcal{I}: \mathbb{R}^n \rightarrow \mathbb{R}$  (convex) :  $\mathcal{I}'(v) = F(v) \quad \forall v \in \mathbb{R}^n$ ,
- $\exists c_1, c_2 > 0$  :  $\mathcal{I}(v) \geq c_1 \|v\| - c_2 \quad \forall v \in \mathbb{R}^n$ .

Assumption  $(\mathcal{A}_3)$  together with  $(\mathcal{A}_1)$  and  $(\mathcal{A}_2)$  have the following consequences:

- $F$  is monotone, i.e.  $(F(u) - F(v), u - v) \geq 0$  for any  $u, v \in \mathbb{R}^n$ .
- $F^o(v)$  is a symmetric and positive semidefinite matrix for any  $v \in \mathbb{R}^n$ .
- The system  $F(u^*) = b$  is equivalent to the following minimization problem:

$$\mathcal{J}(u^*) \leq \mathcal{J}(v) \quad \forall v \in \mathbb{R}^n, \quad \text{where} \quad \mathcal{J}(v) = \mathcal{I}(v) - b^\top v.$$

- The inequality  $\|b\| < c_1$  is a sufficient condition for the existence of the solution  $u^*$ . (It guarantees that the function  $\mathcal{J}$  is coercive in  $\mathbb{R}^n$ .)

Let us complete that the solvability of our system does not hold in general for larger loads unlike problems with unbounded hardening where one can also expect that the operator  $F$  is strongly monotone implying the existence and uniqueness of the solution regardless on  $b$ .

### 3 Limit load method and related limit analysis

The solvability condition  $\|b\| < c_1$  mentioned above is very pessimistic and insufficient for engineering practice. Determination of the so-called *limit load* enables us to find a much more convenient condition for the solvability of  $F(u^*) = b$ . In addition, it enables us to find the factor of safety (FoS) which is important for stability assessment of structures.

### 3.1 Definition of the limit load

In order to define the limit load, it suffices to parametrize our problem using a scalar load factor  $t \geq 0$ :

$$\text{for any } t \geq 0, \text{ find } \hat{u}(t) \in \mathbb{R}^n : F(\hat{u}(t)) = tb. \quad (3.1)$$

The limit load factor will be denoted as  $t_{lim}$  and is naturally defined by

$$t_{lim} = \text{maximum of } t \geq 0 \text{ such that the solution } \hat{u}(t) \text{ of (3.1) exists.} \quad (3.2)$$

More precisely, "supremum" instead of "maximum" should be used in (3.2) because the system (3.1) often does not have a solution for  $t = t_{lim}$ . The case  $t_{lim} = +\infty$  can also occur in some extreme cases, for example if the effective friction and dilatancy angles (see Section 5) are greater than 45 degrees. We have the following consequences of (3.1) and (3.2):

- The system (3.1) has a solution for any  $t < t_{lim}$ , see e.g. [20].
- The system (3.1) has no solution for any  $t > t_{lim}$ .
- If  $t_{lim} > 1$  then the original system  $F(u^*) = b$  has a solution because  $u^* = \hat{u}(1)$ .

In order to determine the unknown value  $t_{lim}$ , it offers to use a direct continuation technique enabling to subsequently increase the load factor  $t$ . Unfortunately, in many cases we observe  $\|\hat{u}(t)\| \rightarrow +\infty$  as  $t \rightarrow t_{lim}$  (see the explanation below) meaning that the small change of  $t$  in vicinity of  $t_{lim}$  can cause very large change of the unknown displacement vector. Therefore, the continuation over  $t$  does not need to be numerically stable.

To explain the behavior of  $\hat{u}(t)$  in vicinity of  $t_{lim}$ , the mapping  $t \mapsto b^\top \hat{u}(t)$  representing the work of external forces was analyzed in [20]. It was shown that this mapping is an increasing and continuous function in the interval  $(0, t_{lim})$  under the assumptions  $(\mathcal{A}_1) - (\mathcal{A}_3)$ , see Figure 1. In addition, if the solution  $\hat{u}(t)$  exists for  $t = t_{lim}$  then the solution  $\hat{u}(t_{lim})$  is not unique and the corresponding solution set is unbounded. However, we usually observe in geotechnical practice that the displacements are unbounded in vicinity of the limit load as in Figure 1.

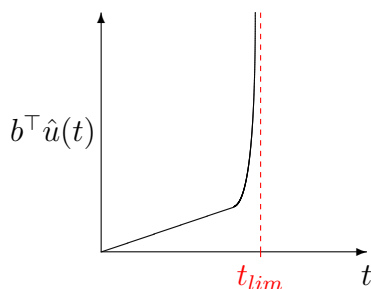


Figure 1: The work of external forces depending on the load factor  $t$ .

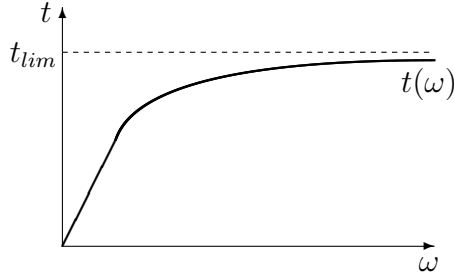


Figure 2: Control of the loading process through the work of external forces.

### 3.2 Continuation method based on the work of external forces

The properties of the mapping  $t \mapsto b^\top \hat{u}(t)$  enables us to introduce a more advanced (indirect) continuation method suggested in [20]. Its idea is to control the loading process through the work of external forces and using the inverse mapping  $\omega \mapsto t(\omega)$  to the original mapping  $t \mapsto b^\top \hat{u}(t)$ , see Figure 2.

We see that the new variable  $\omega$  represents a prescribed value of the work of external forces. Our aim is to find the load factor  $t(\omega)$  and the displacement vector  $\bar{u}(\omega)$  corresponding to a given value of  $\omega \geq 0$ . To this end, the following enriched system of nonlinear equations were proposed in [20]:

$$\text{find } \bar{u}(\omega) \in \mathbb{R}^n, t(\omega) \geq 0 : \quad F(\bar{u}(\omega)) = t(\omega)b, \quad b^\top \bar{u}(\omega) = \omega. \quad (3.3)$$

One can see that the system (3.3) contains one additional linear equation and one additional unknown unlike the system (3.1). The solutions of (3.3) and (3.1) are related as follows

$$\bar{u}(\omega) = \hat{u}(t(\omega)).$$

It is very important to know that the problem (3.3) has a solution for any  $\omega \geq 0$ , the solution component  $t(\omega)$  is unique, the function  $\omega \mapsto t(\omega)$  is continuous, non-decreasing and satisfies  $t(\omega) \rightarrow t_{lim}$ , see [20]. In addition, the solution component  $\bar{u}(\omega)$  also solves the following minimization problem with one linear equality constraint:

$$\mathcal{I}(\bar{u}(\omega)) = \min_{\substack{v \in \mathbb{R}^n \\ b^\top v = \omega}} \mathcal{I}(v), \quad \text{where } \mathcal{I}'(v) = F(v). \quad (3.4)$$

Based on the mentioned properties of the function  $\omega \mapsto t(\omega)$ , one can introduce the following *continuation method for determining  $t_{lim}$* :

1. Generate (adaptively) a sequence  $0 < \omega_1 < \omega_2 < \dots < \omega_N$
2. For any  $j = 1, 2, \dots, N$ , solve the system (3.3) and find its solution  $\bar{u}(\omega_j) \in \mathbb{R}^n, t(\omega_j) \geq 0$ .
3. Approximate  $t_{lim}$  by  $t(\omega_N)$  where  $\omega_N$  is sufficiently large.

We complete this algorithm with the following remarks (recommendations):

- We start with a constant increment of  $\omega$ . Its convenient value can be estimated e.g. using the external work  $b^T u_{el}^*$  of the elastic solution satisfying  $K_{el} u_{el}^* = b$ .
- The increment of  $\omega$  is enlarged (e.g. twice) if the corresponding increments of  $t$  are smaller than a prescribed tolerance (e.g.  $10^{-3}$ ).
- If the increments of  $\omega$  are enlarged several times (e.g. 5 times) then the algorithm is terminated.
- Similar continuation techniques are also known from literature. For example, the loading process can be controlled by a displacement at a selected point (see e.g. [19]) or by the arc-length method [7, 8].

Finally, we introduce the Newton-like method with damping for solving the minimization problem (3.4) for a fixed  $\omega$ :

$$u^{k+1} := u^k + \alpha_k s^k \quad k = 0, 1, \dots, \quad u^0 \text{ given, } b^T u^0 = \omega, \quad (3.5)$$

$$s^k = \arg \min_{\substack{s \in \mathbb{R}^n \\ b^T s = 0}} \left[ \frac{1}{2} (F^o(u^k) s, s) + (F(u^k), s) \right], \quad (3.6)$$

$$\alpha_k = \arg \min_{\alpha \in [0,1]} \mathcal{I}(u^k + \alpha s^k). \quad (3.7)$$

The following remarks provide more details to this algorithm:

- This method can also be interpreted as a sequential quadratic programming. The quadratic functional in (3.6) approximates  $\mathcal{I}$  using the Taylor expansion.
- The initial vector  $u^0$  is achieved by extrapolation from previous two solutions  $\bar{u}(\omega_{j-1})$  and  $\bar{u}(\omega_{j-2})$  corresponding to smaller values of  $\omega$  than the current one.
- The sequence  $\{u^k\}_k$  generated by this algorithm satisfies the constraint  $b^T u^k = \omega$ .
- The vector  $s^k$  is a descent direction of  $\mathcal{I}$ . The minimization problem (3.6) defining  $s^k$  can be transformed to the following system of linear equations:

$$\text{find } s^k \in \mathbb{R}^n, t_k \geq 0 : \quad F^o(u^k) s^k = t_k b - F(u^k), \quad b^T s^k = 0. \quad (3.8)$$

The solution component  $t_k$  is used for approximation of  $t(\omega)$ . This system can be solved by superposition applied on  $F^o(u^k) s^k = t_k b - F(u^k)$ . In particular, we consider the following split of  $s^k$  within the superposition:

$$s^k = v^k + (t_k - t_{0,k}) w^k, \quad \text{where } F^o(u^k) v^k = t_{0,k} b - F(u^k), \quad F^o(u^k) g^k = b$$

and

$$t_{0,k} = \frac{b^T F(u^k)}{\|b\|^2}, \quad t_k = t_{0,k} - \frac{b^T v^k}{b^T w^k}.$$

It is easy to verify that (3.8) is satisfied. Further, we see that two linearized systems of equations with the same stiffness matrix  $F^o(u^k)$  are solved in each Newton's

iteration. One can expect rounding errors within the computation of  $v^k$  and  $w^k$  because the matrix  $F^o(u^k)$  can be ill-posed for higher  $\omega$ . In order to reduce these errors,  $t_{0,k}$  was chosen such that the term  $t_{0,k}b - F(u^k)$  is minimal, i.e. the equality  $b^\top(t_{0,k}b - F(u^k)) = 0$  holds. Alternatively, one could set  $t_{0,k} = t_{k-1}$ .

- If we observe that the matrix  $F^o(u^k)$  is almost singular then we replace it with its regularization in the form  $(1 - \beta)F^o(u^k) + \beta K_{el}$ , where  $\beta \in (0, 1)$  and  $K_{el}$  is the elastic stiffness matrix.
- The damping parameter  $\alpha^k$  is important for global convergence of the algorithm because its presence guarantees that  $\mathcal{I}(u^{k+1}) \leq \mathcal{I}(u^k)$  for any  $k = 0, 1, \dots$ . An alternative line search can be defined, for example, using the Armijo rule:

$$\mathcal{I}(u^k + \alpha_k s^k) - \mathcal{I}(u^k) \leq -\varrho \alpha_k (F^o(u^k) s^k, s^k), \quad \varrho \in (0, 1).$$

It is cheaper to find  $\alpha_k$  satisfying this condition than to solve (3.7). On the other hand, it is not necessary to evaluate the functional  $\mathcal{I}$  if (3.7) is solved.

- Global and local convergence of this algorithm was analyzed in [3]. We usually observe the superlinear convergence in vicinity of the solution. In addition, it is possible to extend this algorithm for contact problems of elasto-plastic bodies, see [20, 3].

### 3.3 Limit analysis problem and its importance

Limit analysis and its lower and upper bounds theorems are well-known methods in stability assessment for many decades because it was originally an analytical method on determining safety factors. Now, it is also a well-established numerical method due to works by R. Temam [25], E. Christiansen [5], S. Sloan [16] and others.

The aim of this subsection is to relate the limit analysis problem with the limit load factor  $t_{lim}$  just by using the continuation method introduced in the previous section. Such an approach was proposed in [3] for the von Mises model and later extended to other elasto-plastic models or to infinite-dimensional (Sobolev's) spaces, see e.g. [10, 11, 12, 21]. Next aim of this section is to highlight importance of the limit analysis problem for computational practice. Some of the results presented below will be introduced without any derivation, for the sake of brevity. Notice that for their derivation, it would be necessary to work with the duality analysis between the static and kinematic principles of elasto-plastic models and thus extend the Assumptions  $(\mathcal{A}_1) - (\mathcal{A}_3)$  from Section 2.

We start with the minimization problem (3.4) having the solution  $\bar{u}(\omega)$  for any  $\omega > 0$  and define the auxiliary vector  $v(\omega) := \bar{u}(\omega)/\omega$ . Then  $v(\omega)$  solves the following minimization problem for given  $\omega > 0$ :

$$\mathcal{I}_\omega(v(\omega)) = \min_{\substack{v \in \mathbb{R}^n \\ b^\top v = 1}} \mathcal{I}_\omega(v), \quad \mathcal{I}_\omega(v) = \frac{1}{\omega} \mathcal{I}(\omega v), \quad \mathcal{I}'(v) = F(v). \quad (3.9)$$

This problem can be easily derived from (3.4) by substitution. We see that the parameter  $\omega$  is not now introduced in the constraint but in the functional. As is justified in [11], it is possible to define the following limit functional:

$$\mathcal{I}_\infty: \mathbb{R}^n \rightarrow \mathbb{R} \cup \{+\infty\}, \quad \mathcal{I}_\infty(v) := \lim_{\omega \rightarrow +\infty} \mathcal{I}_\omega(v), \quad v \in \mathbb{R}^n. \quad (3.10)$$

This functional is in fact the *plastic dissipation function*, which is convex, 1-positively homogeneous, having a linear growth at infinity and is finite-valued only on a closed convex cone  $\mathcal{C} = \{v \in \mathbb{R}^n \mid \mathcal{I}_\infty(v) < +\infty\}$ .

Now, it is quite natural to extend the problem (3.9) for  $\omega = +\infty$  using the functional  $\mathcal{I}_\infty$ . We have the following result:

$$t_{lim} = \inf_{\substack{v \in \mathbb{R}^n \\ b^\top v = 1}} \mathcal{I}_\infty(v) = \min_{\substack{v \in \mathcal{C} \\ b^\top v = 1}} \mathcal{I}_\infty(v). \quad (3.11)$$

The inf-problem is called *kinematic limit analysis problem*. From (3.11), we see that any feasible  $v$  defines an upper bound of  $t_{lim}$ . Therefore, we talk about the upper bound theorem of limit analysis. If the sequence  $\{\bar{u}(\omega)/\omega\}_\omega$  is bounded then its accumulation points are minimizers of  $\mathcal{I}_\infty$ , see [3]. The boundedness of  $\{\bar{u}(\omega)/\omega\}_\omega$  was proven in [3] for the von Mises model.

Although the continuation method presented in Section 3.2 is independent of the limit analysis problem (3.11), its knowledge enriches the computational practice from several reasons:

1. The plastic dissipation  $\mathcal{I}_\infty$  and consequently also the limit load factor  $t_{lim}$  are independent of the elastic material parameters and history of the plastic strain, see Remark 5.1 below. Therefore, it suffices to work with a simplified static version of the elasto-plastic problem (or simply neglect the plastic strain from previous time steps). One can also use fictive elastic parameters to reduce rounding errors. It is helpful if we have high jumps in parameters caused by material heterogeneities or if the Poisson ratio is close to 0.5.
2. There exists an infinite-dimensional counterpart of the problem (3.11) with the same scheme which is defined in terms of displacement rates. It enables us to study convergence of the results with respect to finite element discretization or to describe possible locking effects. For example, if the von Mises model is considered then the constraint set  $\mathcal{C}$  contains divergence free rates of displacements. It is well-known that such constraints cause locking effects if the simplest P1 elements are used. It leads to overestimation of  $t_{lim}$ . Therefore, higher-order elements are recommended within stability analysis. For reliable computation of  $t_{lim}$  using the standard finite elements, functional a-posteriori error estimates of  $t_{lim}$  were developed in [15, 12, 21].
3. To find the minimum of  $\mathcal{I}_\infty$  on infinite-dimensional spaces, it is necessary to extend the Sobolev  $H^1$  space into the BD space [25]. Functions belonging to the BD space can be discontinuous along certain surfaces. It explains from the mathematical point of view the presence of failure zones appearing for the limit load and causing the



plastic collapse of the investigated body. Estimation of these zones is another task within the stability assessment.

4. The BD space can be also discretized by more advanced finite elements allowing certain discontinuities, see [16] and the references therein. It is also very useful to solve the dual problem of limit analysis in terms of stresses leading to a lower bounds of  $t_{lim}$ , see [25, 5, 16, 21]. These advanced methods are out of the scope of this paper but it is worth-mentioning that they were implemented within several SW libraries, e.g., OPTUM-G2 [14].

## 4 Shear strength reduction method

The limit load method and related limit analysis are very universal and can be used in civil or mechanical engineering. However, they are not too conventional in slope stability assessment where another approaches like the limit equilibrium method or the shear strength reduction method (SSRM) are preferred.

The aim of this section is to explain an idea of SSRM within the algebraic level, relate this method to the limit load approach and suggest appropriate algorithmic solutions. More details which are essential for a precise definition of SSRM will be provided in the next section. We refer to [1, 2, 6, 9, 13, 29] for the development of SSRM.

First of all, it is worth mentioning that SSRM is applied only on rock or soil materials with different behavior in compression and in tension. The corresponding plastic models are based, for example, on the Mohr-Coulomb yield criterion introduced in Section 5. Such models contain strength parameters like effective cohesion, effective friction angle or dilatancy angle. The idea is to reduce these parameters until a collapse of the structure occurs.

From the numerical point of view, it means that we use another parametrization of the system (2.2) than in Section 3. In particular, we consider a scalar factor  $\lambda > 0$  and related systems of vector-valued functions  $\{F_\lambda\}_\lambda$  such that the original function  $F$  corresponds to  $\lambda = 1$ . Since  $\lambda$  only changes the strength parameters, it is natural to extend the assumptions  $(\mathcal{A}_1) - (\mathcal{A}_3)$  for the functions  $F_\lambda$  and denote its generalized derivative and potential by  $F_\lambda^o$  and  $\mathcal{I}_\lambda$ , respectively. The parametrized problem reads:

$$\text{for any } \lambda > 0, \text{ find } \tilde{u}(\lambda) \in \mathbb{R}^n : \quad F_\lambda(\tilde{u}(\lambda)) = b, \quad (4.1)$$

or equivalently,

$$\mathcal{J}_\lambda(\tilde{u}(\lambda)) \leq J_\lambda(v) \quad \forall v \in \mathbb{R}^n, \quad \mathcal{J}_\lambda(v) := \mathcal{I}_\lambda(v) - b^\top v. \quad (4.2)$$

For other considerations, we need to add the following assumptions on the system  $\{F_\lambda\}_\lambda$ :

$(\mathcal{A}_4)$  If the system (4.1) has a solution for some  $\bar{\lambda} > 0$  then it has a solution for any  $\lambda \in (0, \bar{\lambda})$ . In addition, we assume that this property holds for any load vector  $b$ .

$(\mathcal{A}_5)$  The function  $\lambda \mapsto F_\lambda(v)$  is continuous for any  $v \in \mathbb{R}^n$ .

Now, we can define the safety factor  $\lambda^*$  for SSRM as follows:

$$\lambda^* = \text{maximum of } \lambda > 0 \text{ such that the solution } \tilde{u}(\lambda) \text{ of (4.1) exists.} \quad (4.3)$$

To find  $\lambda^*$  one can subsequently increase  $\lambda$ . However, similarly as for the limit load, a small change of  $\lambda$  in vicinity of  $\lambda^*$  can cause very large change of  $\tilde{u}(\lambda)$  since we expect that the sequence  $\{\tilde{u}(\lambda)\}_{\lambda < \lambda^*}$  is unbounded. Therefore, we suggest more advanced techniques on determining  $\lambda^*$ .

#### 4.1 Iterative limit load approach for SSRM

The first possible approach how to determine  $\lambda^*$  is to use the framework from Section 3. To this end, for any fixed  $\lambda > 0$ , we consider the following parametrized system with respect to the load factor  $t$ :

$$\text{for any } t \geq 0, \text{ find } \bar{u}_\lambda(t) \in \mathbb{R}^n : \quad F_\lambda(\bar{u}_\lambda(t)) = tb. \quad (4.4)$$

Consequently, we find the corresponding limit load factor and denote it as  $\ell(\lambda) > 0$  to highlight the dependence  $\lambda$ . Clearly, if  $\lambda = 1$  then  $\ell(\lambda) = t_{lim}$ , see Figure 3. We have the following result inspired by [22, 23].

**Lemma 4.1.** *Let the assumptions  $(\mathcal{A}_1) - (\mathcal{A}_5)$  hold for the functions  $F_\lambda$ ,  $\lambda > 0$ . Then the function  $\ell: \lambda \mapsto \ell(\lambda)$  defined above is continuous and non-increasing. In addition, the safety factor  $\lambda^*$  for SSRM is a solution of the equation  $\ell(\lambda^*) = 1$ , see Figure 3.*

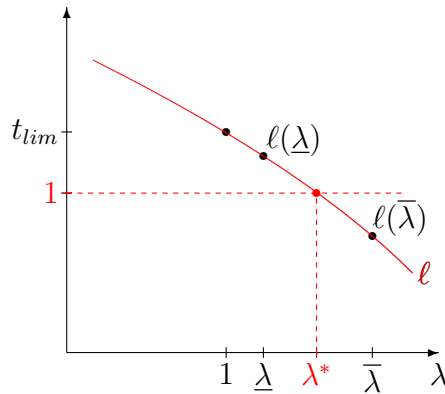


Figure 3: Visualization of the function  $\ell$  and the relationship between the limit load and SSRM safety factors.

*Proof.* Let  $\lambda$  and  $\bar{\lambda}$  be given factors satisfying  $0 < \lambda < \bar{\lambda} < \lambda^*$ . To prove that  $\ell$  is a non-increasing function, it suffices to show that the following inclusion holds: if  $t < \ell(\bar{\lambda})$  then  $t \leq \ell(\lambda)$ . Indeed, if  $t < \ell(\bar{\lambda})$  then the system  $F_{\bar{\lambda}}(\bar{u}_{\bar{\lambda}}(t)) = tb$  has a solution. From the assumption  $(\mathcal{A}_4)$ , it follows that the system  $F_\lambda(\bar{u}_\lambda(t)) = tb$  has also a solution. Using the definition  $\ell(\lambda)$ , we obtain  $t \leq \ell(\lambda)$ . The continuity of  $\ell$  follows from  $(\mathcal{A}_1)$  and  $(\mathcal{A}_5)$ .

If  $\ell(\underline{\lambda}) > 1$  for some  $\underline{\lambda} > 0$ , then the system (4.4) has the solution  $\bar{u}_{\underline{\lambda}}(t)$  for  $t = 1$ . Hence,  $\bar{u}(\underline{\lambda}) = \bar{u}_{\underline{\lambda}}(1)$  is also the solution of (4.1) implying  $\underline{\lambda} \leq \lambda^*$  (see the definition (4.3) of  $\lambda^*$ ). If  $\ell(\bar{\lambda}) > 1$  for some  $\bar{\lambda} > 0$ , then the system (4.4) has no solution for  $t = 1$ . Hence, (4.1) also has no solution implying  $\bar{\lambda} \geq \lambda^*$ . Since the values  $\underline{\lambda}$  and  $\bar{\lambda}$  were chosen arbitrary and  $\ell$  is a continuous function, we obtain  $\ell(\lambda^*) = 1$  as is depicted in Figure 3.  $\square$

We have shown that the safety factor  $\lambda^*$  can be found as a solution of the implicit equation  $\ell(\lambda^*) = 1$ . This equation can be solved by an iterative procedure where a sequence  $\lambda_0, \lambda_1, \dots, \lambda_k, \dots$  is generated and the limit load method is used in each iteration to compute the value  $\ell(\lambda_k)$ ,  $k = 0, 1, \dots$ . In addition, the fact that  $\ell$  is non-increasing enables us to decide whether  $\lambda_k$  is a lower or upper bound of  $\lambda^*$ . We arrive at the following basic algorithm (*iterative limit analysis*) which is inspired by [16, 26, 27, 28].

1. Set  $\epsilon = 0.001$ ,  $k = 0$ ,  $\delta\lambda = 0.1$ ,  $\lambda_k = 1$  and determine  $\ell(\lambda_k)$ .
2. If  $\ell(\lambda_k) > 1 + \epsilon$ , set  $\lambda_{min} = \lambda_k$  (a lower bound of  $\lambda^*$ ) and find  $\lambda_{max}$  (an upper bound of  $\lambda^*$ ) by subsequent increasing of  $\lambda$ , that is,  $\lambda_{k+1} = \lambda_k + \delta\lambda$ . (During the subsequent increasing of  $\lambda$ , it is also possible to update  $\lambda_{min}$ .)
3. If  $\ell(\lambda_k) < 1 - \epsilon$ , set  $\lambda_{max} = \lambda_k$  and find  $\lambda_{min}$  by subsequent decreasing of  $\lambda$ , that is,  $\lambda_{k+1} = \lambda_k - \delta\lambda$ . (During the subsequent decreasing of  $\lambda$ , it is also possible to update  $\lambda_{max}$ .)
4. After finding  $\lambda_{min}$  and  $\lambda_{max}$  (where  $\lambda_{max} - \lambda_{min} = \delta\lambda$ ), we apply the secant method with the following step:

$$\lambda_{k+1} = \lambda_{min} + \frac{\ell(\lambda_{min}) - 1}{\ell(\lambda_{min}) - \ell(\lambda_{max})}(\lambda_{max} - \lambda_{min}).$$

5. Stopping criterion: if  $|\ell(\lambda_k) - 1| \leq \epsilon$  then  $\lambda^* \approx \lambda_k$ .

Let us note that this algorithm is robust and independent of a particular solver of the limit load method. On the other hand, if we consider a solver introduced in Section 3.2 then it is possible to accelerate this algorithm such that we apply the continuation over  $\omega$  only during the first steps where the values  $\lambda_{min}$  and  $\lambda_{max}$  are determined. Within the secant method (where  $\ell(\lambda_{k+1})$  is evaluated), it suffices to let the maximal value of  $\omega$  fixed and initiate the system (3.3) using the solution achieved within the computation of  $\ell(\lambda_k)$ .

## 4.2 Limit problem for SSRM and its regularization

In Section 3.3, we have derived the limit analysis problem for the limit load method using the cost function  $\mathcal{I}_{\infty}$ . In [13, 22], it was shown that a similar *kinematic limit problem for SSRM* exists and reads as follows:

$$\lambda^* = \sup_{\lambda \geq 0} \left\{ \lambda + \inf_{v \in \mathbb{R}^n} \left[ \mathcal{I}_{\infty, \lambda}(v) - b^{\top} v \right] \right\}, \quad (4.5)$$

where

$$\mathcal{I}_{\infty,\lambda}(v) = \lim_{\omega \rightarrow +\infty} \mathcal{I}_{\omega,\lambda}(v), \quad \mathcal{I}_{\omega,\lambda}(v) = \frac{1}{\omega} \mathcal{I}_{\lambda}(\omega v), \quad \mathcal{I}'_{\lambda}(v) = F_{\lambda}(v), \quad \forall v \in \mathbb{R}^n. \quad (4.6)$$

The problem (4.5) is important for deeper analysis of the safety factor  $\lambda^*$  as was shown in [22]. In addition, an advanced numerical method for determining  $\lambda^*$  was introduced there using a regularization of (4.5). Here, we summarize the regularization method and then suggest an algorithm on determining  $\lambda^*$  improving the one presented in [22, 23].

To regularize the problem, it suffices to replace the function  $\mathcal{I}_{\infty,\lambda}$  with  $\mathcal{I}_{\infty,\omega}$ . Then, we arrive at the following approximation of (4.5):

$$\lambda_{\omega} = \sup_{\lambda \geq 0} \{\lambda + G_{\omega}(\lambda)\}, \quad G_{\omega}(\lambda) = \inf_{v \in \mathbb{R}^n} [\mathcal{I}_{\omega,\lambda}(v) - b^{\top} v]. \quad (4.7)$$

It is easy to derive that  $\lambda_{\omega} \leq \lambda^*$  and  $\lambda_{\omega} \rightarrow \lambda^*$  as  $\omega \rightarrow +\infty$ . Further, a vector  $v_{\omega,\lambda}$  is a solution of the inf-problem in (4.7) if and only if it solves the following system of non-linear equations:

$$F_{\lambda}(\omega v_{\omega,\lambda}) = b. \quad (4.8)$$

Comparing (4.1) and (4.8), we obtain  $\omega v_{\omega,\lambda} = \tilde{u}(\lambda)$ . In addition, if  $\lambda < \lambda^*$  then this solution exists (as follows from the definition of  $\lambda^*$ ) and satisfies

$$G_{\omega}(\lambda) = [\mathcal{I}_{\omega,\lambda}(v_{\omega,\lambda}) - b^{\top} v_{\omega,\lambda}] = \frac{1}{\omega} G_1(\lambda), \quad G_1(\lambda) := \mathcal{J}_{\lambda}(\tilde{u}(\lambda)) = \mathcal{I}_{\lambda}(\tilde{u}(\lambda)) - b^{\top} \tilde{u}(\lambda). \quad (4.9)$$

Therefore, the value  $G_{\omega}(\lambda)$  is inversely proportional to the parameter  $\omega$  for any  $\lambda \geq 0$ . Further, there exists  $\bar{\lambda}_{\omega} \geq 0$  satisfying  $\lambda_{\omega} \leq \bar{\lambda}_{\omega} \leq \lambda^*$  and

$$\lambda_{\omega} = \sup_{\lambda \geq 0} \{\lambda + G_{\omega}(\lambda)\} = \bar{\lambda}_{\omega} + G_{\omega}(\bar{\lambda}_{\omega}). \quad (4.10)$$

From (4.9), it also follows that the function  $\omega \mapsto \bar{\lambda}_{\omega}$  is non-decreasing. In addition,  $\bar{\lambda}_{\omega} \rightarrow \lambda^*$  as  $\omega \rightarrow +\infty$ . The situation is depicted in Figure 4.

From the properties of the regularized problem mentioned above, it offers two different strategies how to determine  $\lambda^*$ : 1) use a fixed and sufficiently large value of  $\omega$  to approximate  $\lambda^*$  by  $\bar{\lambda}_{\omega}$ ; 2) generate an increasing sequence  $\{\omega_j\}_{j=1}^N$ , compute  $\bar{\lambda}_{\omega_j}$  for any  $j$  and approximate  $\lambda^*$  by  $\bar{\lambda}_{\omega_N}$ . The first approach was used in [22, 23] where it was shown on several numerical examples that  $\bar{\lambda}_{\omega}$  is close to  $\lambda^*$  even for relatively small  $\omega$ . On the other hand, it was observed there that  $\lambda_{\omega}$  is a good approximation of  $\lambda^*$  only for very large  $\omega$ . The second approach is more time consuming but it can lead to more accurate approximation of  $\lambda^*$ . In addition, the continuation over  $\omega$  can be similar to the one presented in Section 3.2.

#### Algorithm for given $\omega$ :

##### 1. Initialization:

- Set, e.g.,  $\lambda_0 = 0.8$ ,  $\lambda_1 = 0.9$ ,  $\delta\lambda = 0.1$

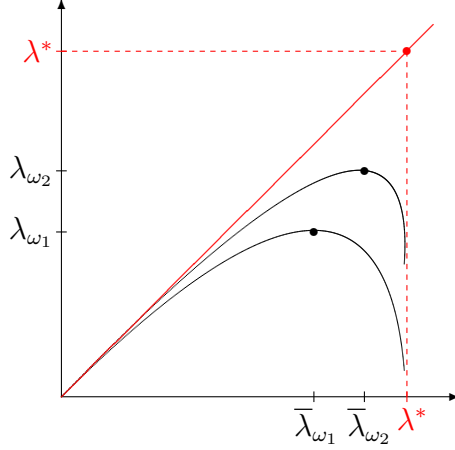


Figure 4: Visualization of the function  $\lambda \mapsto \lambda + G_\omega(\lambda)$  for  $\omega := \omega_1$  and  $\omega := \omega_2$ ,  $\omega_1 < \omega_2$ . The straight line (in red) corresponds to the limit case  $\omega = +\infty$ .

- Solve  $F_{\lambda_0}(\tilde{u}(\lambda_0)) = b$  by the semismooth Newton method with damping, i.e.,

$$u^{j+1} = u^j + \alpha_j s^j, \quad F_{\lambda_0}^o(u^j) s^j = b - F_{\lambda_0}(u^j), \quad \alpha_j = \arg \min_{\alpha \in [0,1]} \mathcal{J}_{\lambda_0}(u^j + \alpha s^j)$$

(One can assume in geotechnics that the system has a solution for  $\lambda_0 = 0.8$ .)

- Compute  $G_1(\lambda_0) = \mathcal{J}_{\lambda_0}(\tilde{u}(\lambda_0))$  and  $H_\omega(\lambda_0) = \lambda_0 + G_\omega(\lambda_0) = \lambda_0 + \frac{1}{\omega} G_1(\lambda_0)$

2. For any  $k = 1, 2, \dots$ :

- Solve  $F_{\lambda_k}(\tilde{u}(\lambda_k)) = b$  by the semismooth Newton method with damping
- If the method does not converge, set  $\lambda_k := (\lambda_{k-1} + \lambda_k)/2$ ,  $\delta\lambda := \delta\lambda/2$  and solve the system above again with updated  $\lambda_k$ . Otherwise, continue with the next step.
- Compute  $G_1(\lambda_k) = \mathcal{J}_{\lambda_k}(\tilde{u}(\lambda_k))$  and  $H_\omega(\lambda_k) = \lambda_k + G_\omega(\lambda_k) = \lambda_k + \frac{1}{\omega} G_1(\lambda_k)$
- If  $H_\omega(\lambda_k) \leq H_\omega(\lambda_{k-1})$  then terminate the algorithm and approximate  $\lambda^*$  with  $\lambda_k$ . Otherwise, continue with the next step.
- Construct the polynomial function  $\lambda \mapsto \tilde{H}_\omega(\lambda)$  which interpolates the values  $H_\omega(\lambda_0), H_\omega(\lambda_1), \dots, H_{\omega,k}(\lambda_k)$ .
- Find  $\lambda_{k+1}$  maximizing  $\tilde{H}_{\omega,k}(\lambda)$  in  $[\lambda_k, \lambda_k + \delta\lambda]$  and then set  $\delta\lambda = \lambda_{k+1} - \lambda_k$ .

We complete this algorithm with the following remarks:

- It is not necessary to find the value  $\bar{\lambda}_\omega$  maximizing the function  $H_\omega$ . It suffices to find its upper bound  $\lambda_k$  for which  $H(\lambda_k) > -\infty$ . Then, we know from our theoretical results that  $\bar{\lambda}_\omega \leq \lambda_k \leq \lambda^*$ .
- In each iteration, we solve the system  $F_{\lambda_k}(\tilde{u}(\lambda_k)) = b$ . However, this system does not need a solution, in general. This is a drawback of this method in comparison

with the iterative limit analysis approach. On the other hand, due to the damping, the sequence  $\{u^j\}_j$  satisfies  $\mathcal{J}_\lambda(u^0) \geq \mathcal{J}_\lambda(u^1) \geq \mathcal{J}_\lambda(u^2) \geq \dots$ . If we observe that  $\mathcal{J}_\lambda(u^j) \ll G_1(\lambda_{k-1})$  then it is possible to terminate the Newton method with unsuccessful convergence.

- The Newton method can be initiated using the solutions from previous steps  $k-1, k-2, \dots$
- It holds that  $H_\omega(\lambda_0) \leq H_\omega(\lambda_1) \leq \dots \leq H_\omega(\lambda_{k-1})$  if the  $k$ -th step is investigated. Further, one can expect that the interpolation  $\tilde{H}_{\omega,k}$  is increasing and concave in  $(\lambda_0, \lambda_k)$ , see Figure 4.
- Let  $\lambda_0, \lambda_1, \dots, \lambda_N$  be a sequence generated by this algorithm for given  $\omega$ . Since the corresponding values  $G_1(\lambda_k)$ ,  $k = 0, 1, \dots, N$  are independent of  $\omega$  they can be also used if we apply this algorithm for some  $\bar{\omega} > \omega$ . It only suffices to update the values  $H_{\bar{\omega}}(\lambda_k) = \lambda_k + \frac{1}{\bar{\omega}}G_1(\lambda_k)$ . Therefore, the continuation over  $\omega$  is not too expensive. We skip its detail, for the sake of brevity.

## 5 Mohr-Coulomb elastic-perfectly plastic model

The main aim of this section is to briefly summarize the construction of constitutive elastoplastic operators which are essential for assembling of the functions  $\mathcal{I}$ ,  $F$ ,  $F^o$  introduced in Section 2. We focus on the Mohr-Coulomb elastic-perfectly plastic model, for illustration. We also explain some details which are beyond the algebraic settings of the problems introduced in previous sections.

### 5.1 Abstract scheme of the elastic-perfectly plastic constitutive problem

Comparing the equations (2.1) with (2.2), we see that the construction of  $F$  depends mainly on the knowledge of the operator  $T: \boldsymbol{\varepsilon} \mapsto \boldsymbol{\sigma}$  where  $\boldsymbol{\varepsilon}$ ,  $\boldsymbol{\sigma}$  denote the small strain tensor and the Cauchy stress tensor, respectively. This mapping is usually defined implicitly, using a time-discretized elastic-perfectly plastic constitutive problem. Its abstract form reads [8, 19]:

Given  $\boldsymbol{\varepsilon}, \boldsymbol{\varepsilon}^p \in \mathbb{R}_{sym}^{3 \times 3}$ , find  $\boldsymbol{\sigma} \in \mathbb{R}_{sym}^{3 \times 3}$ ,  $\boldsymbol{\mu} \in \mathbb{R}_{sym}^{3 \times 3}$  and  $\gamma \in \mathbb{R}$  satisfying:

$$\left. \begin{aligned} \boldsymbol{\sigma} &= \mathbb{D}_e(\boldsymbol{\varepsilon} - \boldsymbol{\varepsilon}^p - \gamma \boldsymbol{\nu}), & \boldsymbol{\nu} &\in \partial g(\boldsymbol{\sigma}), \\ \gamma &\geq 0, & f(\boldsymbol{\sigma}) &\leq 0, & \gamma f(\boldsymbol{\sigma}) &= 0. \end{aligned} \right\} \quad (5.1)$$

Here,  $\boldsymbol{\varepsilon}^p$  denotes the plastic strain from the previous time step,  $\gamma$  is the plastic multiplier,  $\mathbb{D}_e$  is the fourth-order elastic tensor representing the Hooke's law,  $f, g$  are given convex functions representing a yield criterion and a plastic potential, respectively,  $\partial g(\boldsymbol{\sigma})$  denotes the subdifferential of  $g$  at  $\boldsymbol{\sigma}$  and  $\boldsymbol{\nu}$  is an element belonging to  $\partial g(\boldsymbol{\sigma})$ . If  $g$  is differentiable at  $\boldsymbol{\sigma}$  then  $\partial g(\boldsymbol{\sigma})$  is a singleton and thus  $\boldsymbol{\nu} = \partial g(\boldsymbol{\sigma})/\partial \boldsymbol{\sigma}$ . We introduce the Mohr-Coulomb model as a special case of this abstract problem.

## 5.2 The Mohr-Coulomb model and related strength reduction

The Mohr-Coulomb elastic-perfectly plastic model contains 5 material parameters: the bulk modulus,  $K$ , the shear modulus,  $G$ , the (effective) cohesion,  $c$ , the (effective) friction angle,  $\phi$ , and the dilatancy angle,  $\psi$ . Further, this model leads to the following definitions of  $\mathbb{D}_e$ ,  $f$  and  $g$ :

$$\begin{aligned}\mathbb{D}_e \boldsymbol{\varepsilon} &= (K - 2G/3)(\text{tr } \boldsymbol{\varepsilon})\mathbf{I} + 2G\boldsymbol{\varepsilon}, \\ f(\boldsymbol{\sigma}) &= (1 + \sin \phi)\sigma_1 - (1 - \sin \phi)\sigma_3 - 2c \cos \phi, \\ g(\boldsymbol{\sigma}) &= (1 + \sin \psi)\sigma_1 - (1 - \sin \psi)\sigma_3 - 2c \cos \psi,\end{aligned}$$

where  $\text{tr } \boldsymbol{\varepsilon}$  is the trace of  $\boldsymbol{\varepsilon}$ ,  $\mathbf{I}$  denotes the unit second-order tensor and

$$\boldsymbol{\sigma} = \sum_{i=1}^3 \sigma_i e_i \otimes e_i, \quad \sigma_1 \geq \sigma_2 \geq \sigma_3,$$

is the spectral decomposition of  $\boldsymbol{\sigma}$  and thus  $\sigma_1$  and  $\sigma_3$  are the maximal and minimal principle stresses. (We use the standard mechanical sign convention where the tension has a positive sign).

Within the SSRM method introduced in Section 4, the strength parameters  $c$ ,  $\phi$  and  $\psi$  are reduced using the scalar factor  $\lambda > 0$ , for example,

$$c_\lambda := \frac{c}{\lambda}, \quad \phi_\lambda := \arctan \frac{\tan \phi}{\lambda}, \quad \psi_\lambda := \arctan \frac{\tan \psi}{\lambda}. \quad (5.2)$$

It means that the construction of  $F_\lambda$ ,  $F_\lambda^o$  is practically the same as the construction of  $F$ ,  $F^o$ , only different strength parameters are used.

If  $\psi = \phi$  then  $f = g$  and we arrive at the *associated* model with available mathematical theory. In particular, the corresponding algebraic functions  $F$  and  $F_\lambda$  satisfy the required properties  $(\mathcal{A}_1) - (\mathcal{A}_5)$ . If  $\psi \neq \phi$  (mostly we have  $0 \leq \psi < \phi$ ) then we talk about the *non-associated* model. In geotechnics, the non-associated case is more usual than the associated one. However, in such a case, the safety factors for the limit load and SSRM methods are not uniquely defined and numerical methods may oscillate. In addition, the corresponding algebraic function  $F$  is not monotone and thus the crucial assumption  $(\mathcal{A}_3)$  of this paper is not satisfied ( $F$  has not any potential  $\mathcal{I}$  and  $F^o(v)$  is not a symmetric matrix for any  $v$ ).

## 5.3 Approximations of the non-associated model

In order to apply the solution methods introduced in previous sections for the non-associated model, it is necessary to approximate it by the associated model. In case of the limit analysis approach (see Section 3.3), the so-called Davis' approximation was suggested and used e.g. in [16]. Instead of the non-associated model, it is considered the associated model with the following modifications of the parameters  $c$  and  $\phi$ :

$$\bar{c} = \beta c, \quad \bar{\phi} = \bar{\psi} = \arctan(\beta \tan \phi), \quad \beta := \frac{\cos \psi \cos \phi}{1 - \sin \psi \sin \phi}, \quad (5.3)$$

In case of SSRM, the strength parameters  $c$  and  $\phi$  are modified for any factor  $\lambda > 0$ . A general scheme of modified SSRM was introduced in [22]:

$$\tilde{c}_\lambda := \frac{c}{q(\lambda; \phi, \psi)}, \quad \tan \tilde{\phi}_\lambda = \tan \tilde{\psi}_\lambda := \frac{\tan \phi}{q(\lambda; \phi, \psi)}, \quad (5.4)$$

where  $q$  is a scalar function satisfying:

- $q$  is positive and continuous for any  $\lambda > 0$  and any  $\phi', \psi'$  such that  $0 \leq \psi' \leq \phi'$ ;
- $q$  is increasing with respect to the variable  $\lambda \geq 0$ ;
- $q$  is non-increasing with respect to the variable  $\psi' \in [0, \phi']$ ;
- $q(\lambda; \phi', \psi') \geq \lambda$  for any  $\lambda \geq 0$  and any  $\phi', \psi'$  such that  $0 \leq \psi' \leq \phi'$ ;
- if  $\psi' = \phi'$  then  $q(\lambda; \phi', \psi') = \lambda$ .

The following three examples of the function  $q$  was introduced and analyzed in [22]:

$$\begin{aligned} q_A(\lambda; \phi, \psi) &= \lambda \frac{1 - \sin \psi \sin \phi}{\cos \psi \cos \phi}, \\ q_B(\lambda; \phi, \psi) &= \lambda \frac{1 - \sin \psi_\lambda \sin \phi_\lambda}{\cos \psi_\lambda \cos \phi_\lambda}, \quad \phi_\lambda = \arctan \frac{\tan \phi'}{\lambda}, \quad \psi_\lambda = \arctan \frac{\tan \psi'}{\lambda}, \\ q_C(\lambda; \phi, \psi) &= \begin{cases} \lambda \frac{1 - \sin \psi \sin \phi_\lambda}{\cos \psi \cos \phi_\lambda}, & \text{if } \phi_\lambda \geq \psi, \\ \lambda, & \text{if } \phi_\lambda \leq \psi, \end{cases} \quad \phi_\lambda = \arctan \frac{\tan \phi'}{\lambda}. \end{aligned}$$

These functions correspond to the Davis A, B and C approaches suggested in [27, 28].

It is important to emphasize that the presented modifications change only material parameters and thus do not influence the construction of the constitutive operators.

## 5.4 Construction of the constitutive operators for the associated model

The operator  $T : \boldsymbol{\varepsilon} \mapsto \boldsymbol{\sigma}$  defined by (5.1) and its generalized derivative  $T^o$  were constructed in [19, 18] even for a more general Mohr-Coulomb model. From  $T$  and  $T^o$ , one can assemble the functions  $F$  and  $F^o$ , respectively. Since the non-associated model is approximated in our case, it suffices to consider the problem (5.1) with  $g = f$ . In addition, we set there  $\boldsymbol{\varepsilon}^p = \mathbf{0}$  since we expect that the investigated safety factors are independent of the plastic strain history. Under these simplifications, (5.1) is equivalent to the following optimization problem [22]:

$$\Psi_T(\boldsymbol{\varepsilon}) = \max_{\boldsymbol{\tau}, f(\boldsymbol{\tau}) \leq 0} \left[ \boldsymbol{\tau} : \boldsymbol{\varepsilon} - \frac{1}{2} \mathbb{D}_e^{-1} \boldsymbol{\tau} : \boldsymbol{\tau} \right]. \quad (5.5)$$

Here, the Cauchy stress  $\boldsymbol{\sigma}$  maximizes the functional on the right-hand side subject to the constraint  $f(\boldsymbol{\tau}) \leq 0$ . In addition,  $\frac{\partial \Psi_T(\boldsymbol{\varepsilon})}{\partial \boldsymbol{\varepsilon}} = T(\boldsymbol{\varepsilon}) = \boldsymbol{\sigma}$  meaning that the potential  $\mathcal{I}$  defined in Section 2 can be assembled using the function  $\Psi_T$ . Therefore, we also summarize the construction of  $\Psi_T$ , beside  $T$  and  $T^o$ . For more details, we refer to [22, 19, 18].



**Remark 5.1.** It is worth noticing that the function  $\mathcal{I}_\infty$  defined in Section 3.3 can be assembled using the following local dissipation function:

$$\Psi_\infty(\boldsymbol{\varepsilon}) = \sup_{\boldsymbol{\tau}, f(\boldsymbol{\tau}) \leq 0} [\boldsymbol{\tau} : \boldsymbol{\varepsilon}].$$

The supremum is used in this definition because  $\Psi_\infty(\boldsymbol{\varepsilon}) = +\infty$  for some  $\boldsymbol{\varepsilon}$ . We skip the construction of  $\Psi_\infty$  for the sake of brevity.

We assume that the strain tensor  $\boldsymbol{\varepsilon}$  is given and its eigenvalues  $\varepsilon_1, \varepsilon_2, \varepsilon_3$  satisfy  $\varepsilon_1 \geq \varepsilon_2 \geq \varepsilon_3$ . Let  $\text{tr } \boldsymbol{\varepsilon} = \varepsilon_1 + \varepsilon_2 + \varepsilon_3$  denote the trace of  $\boldsymbol{\varepsilon}$  and  $\Lambda = \frac{1}{3}(3K - 2G)$  denote the first Lamé coefficient. As in [8], we distinguish five possible scenarios within the solution of (5.1) according to the unknown stress tensor  $\boldsymbol{\sigma}$  and its principal stresses  $\sigma_1, \sigma_2, \sigma_3$ , see (5.2): the elastic response ( $f(\boldsymbol{\sigma}) \leq 0$ ), the return to the smooth portion of the Mohr-Coulomb pyramid ( $f(\boldsymbol{\sigma}) = 0$  and  $\sigma_1 > \sigma_2 > \sigma_3$ ), the return to the left edge ( $f(\boldsymbol{\sigma}) = 0$  and  $\sigma_1 = \sigma_2 > \sigma_3$ ), the return to the right edge ( $f(\boldsymbol{\sigma}) = 0$  and  $\sigma_1 > \sigma_2 = \sigma_3$ ), and the return to the apex of the pyramid ( $f(\boldsymbol{\sigma}) = 0$  and  $\sigma_1 = \sigma_2 = \sigma_3$ ).

**The elastic response.** This case happens if the elastic stress  $\mathbb{D}_e \boldsymbol{\varepsilon}$  satisfies  $f(\mathbb{D}_e \boldsymbol{\varepsilon}) \leq 0$ , that is,

$$2\Lambda(\text{tr } \boldsymbol{\varepsilon}) \sin \phi + 2G(1 + \sin \phi)\varepsilon_1 - 2G(1 - \sin \phi)\varepsilon_3 - 2c \cos \phi \leq 0. \quad (5.6)$$

Then

$$\begin{aligned} \Psi_T(\boldsymbol{\varepsilon}) &= \frac{1}{2} \mathbb{D}_e \boldsymbol{\varepsilon} : \boldsymbol{\varepsilon} = \frac{1}{2} \Lambda (\text{tr } \boldsymbol{\varepsilon})^2 + G(\varepsilon_1^2 + \varepsilon_2^2 + \varepsilon_3^2), \\ T(\boldsymbol{\varepsilon}) &= \mathbb{D}_e \boldsymbol{\varepsilon}, \quad T^o(\boldsymbol{\varepsilon}) = \mathbb{D}_e. \end{aligned}$$

If the criterion (5.6) does not hold, i.e., if  $f(\mathbb{D}_e \boldsymbol{\varepsilon}) > 0$  then the plastic response occurs and we distinguish four possible cases of the return to the Mohr-Coulomb pyramid. We use the following auxiliary functions to decide which type of the return occurs:

$$\begin{aligned} \gamma_{s,l}(\boldsymbol{\varepsilon}) &= \frac{\varepsilon_1 - \varepsilon_2}{1 + \sin \phi}, & \gamma_{s,r}(\boldsymbol{\varepsilon}) &= \frac{\varepsilon_2 - \varepsilon_3}{1 - \sin \phi}, \\ \gamma_{l,a}(\boldsymbol{\varepsilon}) &= \frac{\varepsilon_1 + \varepsilon_2 - 2\varepsilon_3}{3 - \sin \phi}, & \gamma_{r,a}(\boldsymbol{\varepsilon}) &= \frac{2\varepsilon_2 - \varepsilon_2 - \varepsilon_3}{3 + \sin \phi}. \end{aligned}$$

**The return to the smooth portion.** This case happens if the strain tensor  $\boldsymbol{\varepsilon}$  satisfies

$$f(\mathbb{D}_e \boldsymbol{\varepsilon}) > 0 \quad \text{and} \quad q_s(\boldsymbol{\varepsilon}) < S \min\{\gamma_{s,l}(\boldsymbol{\varepsilon}), \gamma_{s,r}(\boldsymbol{\varepsilon})\}, \quad (5.7)$$

where

$$\begin{aligned} q_s(\boldsymbol{\varepsilon}) &= 2\Lambda(\text{tr } \boldsymbol{\varepsilon}) \sin \phi + 2G(1 + \sin \phi)\varepsilon_1 - 2G(1 - \sin \phi)\varepsilon_3 - 2c \cos \phi, \\ S &= 4\Lambda \sin^2 \phi + 4G(1 + \sin^2 \phi). \end{aligned}$$

It is important to note that the criterion (5.7) can hold only if  $\varepsilon_1 > \varepsilon_2 > \varepsilon_3$ . Therefore, the following auxiliary notation is well-defined:

$$\begin{aligned}\mathbf{E}_i &= \frac{(\boldsymbol{\varepsilon} - \varepsilon_j \mathbf{I})(\boldsymbol{\varepsilon} - \varepsilon_k \mathbf{I})}{(\varepsilon_i - \varepsilon_j)(\varepsilon_i - \varepsilon_k)}, \quad i \neq j \neq k \neq i, \quad i = 1, 2, 3, \\ \mathbf{F}_s &= 2G(1 + \sin \phi) \mathbf{E}_1 - 2G(1 - \sin \phi) \mathbf{E}_3 + 2\Lambda \sin \phi \mathbf{I}, \\ \mathbb{E}_i &= \frac{\mathbb{E}^2 - (\varepsilon_j + \varepsilon_k) \mathbb{I} - (2\varepsilon_i - \varepsilon_j - \varepsilon_k) \mathbf{E}_i \otimes \mathbf{E}_i}{(\varepsilon_i - \varepsilon_j)(\varepsilon_i - \varepsilon_k)} \\ &\quad - \frac{(\varepsilon_j - \varepsilon_k) [\mathbf{E}_j \otimes \mathbf{E}_j - \mathbf{E}_k \otimes \mathbf{E}_k]}{(\varepsilon_i - \varepsilon_j)(\varepsilon_i - \varepsilon_k)}, \quad i \neq j \neq k \neq i, \quad i = 1, 2, 3.\end{aligned}$$

In particular,  $\mathbf{E}_1, \mathbf{E}_2, \mathbf{E}_3$  define the eigenprojections of  $\boldsymbol{\varepsilon}$ , that is,  $\boldsymbol{\varepsilon} = \varepsilon_1 \mathbf{E}_1 + \varepsilon_2 \mathbf{E}_2 + \varepsilon_3 \mathbf{E}_3$ , see [8]. Further, it holds:  $\mathbf{E}_i = \partial \varepsilon_i / \partial \boldsymbol{\varepsilon}$  and  $\mathbb{E}_i = \partial \mathbf{E}_i / \partial \boldsymbol{\varepsilon}$ ,  $i = 1, 2, 3$ . Using this notation, we have:

$$\begin{aligned}\Psi_T(\boldsymbol{\varepsilon}) &= \frac{1}{2} \Lambda (\text{tr } \boldsymbol{\varepsilon})^2 + G(\varepsilon_1^2 + \varepsilon_2^2 + \varepsilon_3^2) - \frac{1}{2S} q_s^2(\boldsymbol{\varepsilon}), \\ T(\boldsymbol{\varepsilon}) &= \sigma_1 \mathbf{E}_1 + \sigma_2 \mathbf{E}_2 + \sigma_3 \mathbf{E}_3, \\ T^o(\boldsymbol{\varepsilon}) &= \sum_{i=1}^3 [\sigma_i \mathbb{E}_i + 2G \mathbf{E}_i \otimes \mathbf{E}_i] + \frac{1}{3} (3K - 2G) \mathbf{I} \otimes \mathbf{I} - \frac{1}{S} \mathbf{F}_s \otimes \mathbf{F}_s,\end{aligned}$$

where

$$\begin{aligned}\sigma_1 &= \Lambda (\text{tr } \boldsymbol{\varepsilon}) + 2G\varepsilon_1 - \frac{2\Lambda \sin \phi + 2G(1 + \sin \phi)}{S} q_s(\boldsymbol{\varepsilon}), \\ \sigma_2 &= \Lambda (\text{tr } \boldsymbol{\varepsilon}) + 2G\varepsilon_2 - \frac{2\Lambda \sin \phi}{S} q_s(\boldsymbol{\varepsilon}), \\ \sigma_3 &= \Lambda (\text{tr } \boldsymbol{\varepsilon}) + 2G\varepsilon_3 - \frac{2\Lambda \sin \phi - 2G(1 - \sin \phi)}{S} q_s(\boldsymbol{\varepsilon}).\end{aligned}$$

**The return to the left edge.** This case happens if the strain tensor  $\boldsymbol{\varepsilon}$  satisfies

$$f(\mathbb{D}_e \boldsymbol{\varepsilon}) > 0, \quad \gamma_{s,l}(\boldsymbol{\varepsilon}) < \gamma_{l,a}(\boldsymbol{\varepsilon}) \quad \text{and} \quad L\gamma_{s,l}(\boldsymbol{\varepsilon}) \leq q_l(\boldsymbol{\varepsilon}) < L\gamma_{l,a}(\boldsymbol{\varepsilon}), \quad (5.8)$$

where

$$\begin{aligned}q_l(\boldsymbol{\varepsilon}) &= 2\Lambda (\text{tr } \boldsymbol{\varepsilon}) \sin \phi + G(1 + \sin \phi)(\varepsilon_1 + \varepsilon_2) - 2G(1 - \sin \phi)\varepsilon_3 - 2c \cos \phi, \\ L &= 4\Lambda \sin^2 \phi + G(1 + \sin \phi)^2 + 2G(1 - \sin \phi)^2.\end{aligned}$$

It is important to note that the criterion (5.8) can hold only if  $\varepsilon_2 > \varepsilon_3$ . Therefore, the following auxiliary notation is well-defined:

$$\begin{aligned}\mathbf{E}_3 &= \frac{(\boldsymbol{\varepsilon} - \varepsilon_1 \mathbf{I})(\boldsymbol{\varepsilon} - \varepsilon_2 \mathbf{I})}{(\varepsilon_3 - \varepsilon_1)(\varepsilon_3 - \varepsilon_2)}, \quad \mathbf{E}_{12} = \mathbf{I} - \mathbf{E}_3, \\ \mathbf{F}_l &= G(1 + \sin \phi) \mathbf{E}_{12} - 2G(1 - \sin \phi) \mathbf{E}_3 + 2\Lambda \sin \phi \mathbf{I}, \\ \mathbb{E}_3 &= \frac{\mathbb{E}^2 - (\varepsilon_1 + \varepsilon_2) \mathbb{I} - [\boldsymbol{\varepsilon} \otimes \mathbf{E}_{12} + \mathbf{E}_{12} \otimes \boldsymbol{\varepsilon}] + (\varepsilon_1 + \varepsilon_2) \mathbf{E}_{12} \otimes \mathbf{E}_{12}}{(\varepsilon_3 - \varepsilon_1)(\varepsilon_3 - \varepsilon_2)} \\ &\quad + \frac{(\varepsilon_1 + \varepsilon_2 - 2\varepsilon_3) \mathbf{E}_3 \otimes \mathbf{E}_3 + \varepsilon_3 [\mathbf{E}_{12} \otimes \mathbf{E}_3 + \mathbf{E}_3 \otimes \mathbf{E}_{12}]}{(\varepsilon_3 - \varepsilon_1)(\varepsilon_3 - \varepsilon_2)}.\end{aligned}$$

The definitions of  $\mathbb{E}_3$  introduced here and in the previous paragraph are equivalent under the assumption  $\varepsilon_1 > \varepsilon_2 > \varepsilon_3$ . The solution scheme for the return to the left edge reads as:

$$\begin{aligned}\Psi_T(\boldsymbol{\varepsilon}) &= \frac{1}{2}\Lambda(\text{tr } \boldsymbol{\varepsilon})^2 + G\left[\frac{1}{2}(\varepsilon_1 + \varepsilon_2)^2 + \varepsilon_3^2\right] - \frac{1}{2L}q_l^2(\boldsymbol{\varepsilon}), \\ T(\boldsymbol{\varepsilon}) &= \sigma_1\mathbf{E}_{12} + \sigma_3\mathbf{E}_3, \\ T^o(\boldsymbol{\varepsilon}) &= (\sigma_3 - \sigma_1)\mathbb{E}_3 + G\mathbf{E}_{12} \otimes \mathbf{E}_{12} + 2G\mathbf{E}_3 \otimes \mathbf{E}_3 + \Lambda\mathbf{I} \otimes \mathbf{I} - \frac{1}{L}\mathbf{F}_l \otimes \mathbf{F}_l,\end{aligned}$$

where

$$\begin{aligned}\sigma_1 = \sigma_2 &= \Lambda(\text{tr } \boldsymbol{\varepsilon}) + G(\varepsilon_1 + \varepsilon_2) - \frac{2\Lambda \sin \phi + G(1 + \sin \phi)}{L}q_l(\boldsymbol{\varepsilon}), \\ \sigma_3 &= \Lambda(\text{tr } \boldsymbol{\varepsilon}) + 2G\varepsilon_3 - \frac{2\Lambda \sin \phi - 2G(1 - \sin \phi)}{L}q_l(\boldsymbol{\varepsilon}).\end{aligned}$$

**The return to the right edge.** This case happens if the strain tensor  $\boldsymbol{\varepsilon}$  satisfies

$$f(\mathbb{D}_e \boldsymbol{\varepsilon}) > 0, \quad \gamma_{s,r}(\boldsymbol{\varepsilon}) < \gamma_{r,a}(\boldsymbol{\varepsilon}) \quad \text{and} \quad R\gamma_{s,r}(\boldsymbol{\varepsilon}) \leq q_r(\boldsymbol{\varepsilon}) < R\gamma_{r,a}(\boldsymbol{\varepsilon}), \quad (5.9)$$

where

$$\begin{aligned}q_r(\boldsymbol{\varepsilon}) &= 2\Lambda(\text{tr } \boldsymbol{\varepsilon}) \sin \phi + 2G(1 + \sin \phi)\varepsilon_1 - G(1 - \sin \phi)(\varepsilon_2 + \varepsilon_3) - 2c \cos \phi, \\ R &= 4\Lambda \sin^2 \phi + 2G(1 + \sin \phi)^2 + G(1 - \sin \phi)^2.\end{aligned}$$

It is important to note that the criterion (5.9) can hold only if  $\varepsilon_1 > \varepsilon_2$ . Therefore, the following auxiliary notation is well-defined:

$$\begin{aligned}\mathbf{E}_1 &= \frac{(\boldsymbol{\varepsilon} - \varepsilon_2\mathbf{I})(\boldsymbol{\varepsilon} - \varepsilon_3\mathbf{I})}{(\varepsilon_1 - \varepsilon_2)(\varepsilon_1 - \varepsilon_3)}, \quad \mathbf{E}_{23} = \mathbf{I} - \mathbf{E}_1, \\ \mathbf{F}_r &= 2G(1 + \sin \phi)\mathbf{E}_1 - G(1 - \sin \phi)\mathbf{E}_{23} + 2\Lambda \sin \phi \mathbf{I}, \\ \mathbb{E}_1 &= \frac{\mathbb{E}^2 - (\varepsilon_2 + \varepsilon_3)\mathbb{I} - [\boldsymbol{\varepsilon} \otimes \mathbf{E}_{23} + \mathbf{E}_{23} \otimes \boldsymbol{\varepsilon}] + (\varepsilon_2 + \varepsilon_3)\mathbf{E}_{23} \otimes \mathbf{E}_{23}}{(\varepsilon_1 - \varepsilon_2)(\varepsilon_1 - \varepsilon_2)} \\ &\quad + \frac{(\varepsilon_2 + \varepsilon_3 - 2\varepsilon_1)\mathbf{E}_1 \otimes \mathbf{E}_1 + \varepsilon_1[\mathbf{E}_{23} \otimes \mathbf{E}_1 + \mathbf{E}_1 \otimes \mathbf{E}_{23}]}{(\varepsilon_1 - \varepsilon_2)(\varepsilon_1 - \varepsilon_3)}.\end{aligned}$$

The definitions of  $\mathbb{E}_1$  introduced here and for the return to the smooth portion are equivalent under the assumption  $\varepsilon_1 > \varepsilon_2 > \varepsilon_3$ . The solution scheme for the return to the right edge reads as:

$$\begin{aligned}\Psi_T(\boldsymbol{\varepsilon}) &= \frac{1}{2}\Lambda(\text{tr } \boldsymbol{\varepsilon})^2 + G\left[\varepsilon_1^2 + \frac{1}{2}(\varepsilon_2 + \varepsilon_3)^2\right] - \frac{1}{2R}q_r^2(\boldsymbol{\varepsilon}), \\ T(\boldsymbol{\varepsilon}) &= \sigma_1\mathbf{E}_1 + \sigma_3\mathbf{E}_{23}, \\ T^o(\boldsymbol{\varepsilon}) &= (\sigma_1 - \sigma_3)\mathbb{E}_1 + 2G\mathbf{E}_1 \otimes \mathbf{E}_1 + G\mathbf{E}_{23} \otimes \mathbf{E}_{23} + \Lambda\mathbf{I} \otimes \mathbf{I} - \frac{1}{R}\mathbf{F}_r \otimes \mathbf{F}_r,\end{aligned}$$

where

$$\begin{aligned}\sigma_1 &= \Lambda(\operatorname{tr} \boldsymbol{\varepsilon}) + 2G\varepsilon_1 - \frac{2\Lambda \sin \phi + 2G(1 + \sin \phi)}{L} q_l(\boldsymbol{\varepsilon}), \\ \sigma_3 = \sigma_2 &= \Lambda(\operatorname{tr} \boldsymbol{\varepsilon}) + G(\varepsilon_2 + \varepsilon_3) - \frac{2\Lambda \sin \phi - G(1 - \sin \phi)}{L} q_l(\boldsymbol{\varepsilon}).\end{aligned}$$

**The return to the apex.** This case happens if the strain tensor  $\boldsymbol{\varepsilon}$  satisfies

$$f(\mathbb{D}_e \boldsymbol{\varepsilon}) > 0 \quad \text{and} \quad q_a(\boldsymbol{\varepsilon}) \geq A \max\{\gamma_{l,a}(\boldsymbol{\varepsilon}), \gamma_{r,a}(\boldsymbol{\varepsilon})\}, \quad (5.10)$$

where

$$q_a(\boldsymbol{\varepsilon}) = 2K(\operatorname{tr} \boldsymbol{\varepsilon}) \sin \phi - 2c \cos \phi, \quad A = 4K \sin^2 \phi.$$

Then,

$$\begin{aligned}\Psi_T(\boldsymbol{\varepsilon}) &= \frac{1}{2}K(\operatorname{tr} \boldsymbol{\varepsilon})^2 - \frac{1}{2A}q_a^2(\boldsymbol{\varepsilon}) = \frac{c}{\tan \phi}(\operatorname{tr} \boldsymbol{\varepsilon}) - \frac{c^2}{2K \tan^2 \phi}, \\ T(\boldsymbol{\varepsilon}) &= \sigma_1 \mathbf{I}, \quad \sigma_1 = \sigma_2 = \sigma_3 = \frac{c}{\tan \phi}, \\ T^o(\boldsymbol{\varepsilon}) &= 0.\end{aligned}$$

## 6 Notes to the implementation in Matlab

For the implementation of the suggested algorithms, we plan to extend our in-house elastoplastic codes in Matlab which are described in [4] and available for download. Similar codes were also used, e.g., in [19, 12, 22, 23] within the limit load and SSRM methods. They are based on standard finite element methods.

Currently, the code for the algorithm from Section 4.1 is available for download in [24].

## References

- [1] Brinkgreve, R.B.J. and Bakker, H.L. Non-linear finite element analysis of safety factors. *Proceedings of the international conference on computer methods and advances in geomechanics*. Rotterdam, the Netherlands: Balkema. (1991) 1117–1122.
- [2] Brinkgreve, R.B.J., Swolfs, W.M. and Engin, E. *Plaxis 2D 2011 – user manual*. Delft, the Netherlands: Plaxis bv. (2011).
- [3] M. Čermák, J. Haslinger, T. Kozubek, S. Sysala: Discretization and numerical realization of contact problems for elastic-perfectly plastic bodies. PART II - numerical realization, limit analysis. *ZAMM* 95, 2015, pages 1348-1371.
- [4] Čermák, M., Sysala, S. and Valdman, J. Efficient and flexible MATLAB implementation of 2D and 3D elastoplastic problems. *Applied Mathematics and Computation* **355** (2019) 595–614.

- [5] Christiansen, E. *Limit analysis of collapse states*. In P. G. Ciarlet and J. L. Lions, editors, *Handbook of Numerical Analysis*, Vol IV, Part 2, North-Holland, (1996) 195–312.
- [6] Dawson, E.M., Roth, W.H. and Drescher, A.A. (1999). Slope stability analysis by strength reduction. *Géotechnique* **49** (1999) 835–840
- [7] R. de Borst, M.A. Crisfield, J.J.C. Remmers, C.V. Verhoosel, *Non-Linear Finite Element Analysis of Solids and Structures* (Wiley-Blackwell, 2012).
- [8] E.A. de Souza Neto, D. Perić, D.R.J. Owen, *Computational Methods for Plasticity* (Wiley-Blackwell, 2008).
- [9] Griffiths, D.V. & Lane, P.A. . Slope stability analysis by finite elements. *Géotechnique* **49** (1999) 387–403.
- [10] Haslinger, J., Repin and S., Sysala, S. A reliable incremental method of computing the limit load in deformation plasticity based on compliance: Continuous and discrete setting. *Journal of Computational and Applied Mathematics* **303** (2016) 156–170.
- [11] Haslinger, J., Repin, S. and Sysala, S. Guaranteed and computable bounds of the limit load for variational problems with linear growth energy functionals. *Applications of Mathematics* **61** (2016) 527–564.
- [12] Haslinger, J., Repin, S. and Sysala, S. Inf-sup conditions on convex cones and applications to limit load analysis. *Mathematics and Mechanics of Solids* **24** (2019) 3331–3353.
- [13] Krabbenhoft, K. and Lyamin, A.V. Strength reduction finite-element limit analysis. *Géotechnique Letters* **5** (2015) 250–253.
- [14] Krabbenhoft, K., Lyamin, A. and Krabbenhoft, J. *OptumG2: theory*. Newcastle, Australia: Optum Computational Engineering, (2016).
- [15] Repin, S., Sysala, S. and Haslinger, J. Computable majorants of the limit load in Hencky’s plasticity problems. *Comp. & Math. with Appl.* **75** (2018) 199–217.
- [16] Sloan, S.W. Geotechnical stability analysis, *Géotechnique*, **63** (2013) 531–572.
- [17] D. Sun: A further result on an implicit function theorem for locally Lipschitz function. *Oper. Res. Lett.* **28** (2001), 193–198.
- [18] S. Sysala, M. Čermák: Implicit constitutive solution scheme for Mohr-Coulomb plasticity. In: J. Chleboun, P. Kůs, P. Příkryl, K. Segeth, J. Šístek, T. Vejchodský (eds.): *Programs and Algorithms of Numerical Mathematics*. Proceedings of Seminar, Institute of Mathematics CAS, Prague, 2017, pages 120-129.
- [19] Sysala, S., Čermák, M. and Ligurský, T. Subdifferential-based implicit return-mapping operators in Mohr-Coulomb plasticity. *ZAMM* **97** (2017) 1502–1523.

- [20] Sysala, S., Haslinger, J., Hlaváček, I. and Cermak, M. Discretization and numerical realization of contact problems for elastic-perfectly plastic bodies. PART I–discretization, limit analysis. *ZAMM* **95** (2015) 333–353.
- [21] Sysala, S., Haslinger, J., Reddy, B.D. and Repin, S. An abstract inf-sup problem inspired by limit analysis in perfect plasticity and related applications. *Mathematical Models and Methods in Applied Sciences*. To appear in 2021, <http://arxiv.org/abs/2009.03535>.
- [22] Sysala, S., Hrubesova, E., Michalec, Z. and Tschuchnigg, F. Optimization and variational principles for the shear strength reduction method. *International Journal for Numerical and Analytical Methods in Geomechanics* **45** (2021) 2388-2407.
- [23] S. Sysala, F. Tschuchnigg, E. Hrubesová, Z. Michalec: Optimization variant of the shear strength reduction method and its usage for stability of embankments with unconfined seepage. *Computers and Structures* 281, 2023, 107033.
- [24] S. Sysala: Matlab codes on the iterative limit load approach within the shear strength reduction method, <https://github.com/sysala/SSRM> .
- [25] R. Temam, *Mathematical Problems in Plasticity* (Paris, 1985).
- [26] Tschuchnigg, F., Schweiger, H.F., Sloan, S.W., Lyamin, A.V. and Raissakis, I. Comparison of finite-element limit analysis and strength reduction techniques. *Géotechnique* **65** (2015) 249–257.
- [27] Tschuchnigg, F., Schweiger, H.F. and Sloan, S.W. Slope stability analysis by means of finite element limit analysis and finite element strength reduction techniques. Part I: Numerical studies considering non-associated plasticity. *Computers and Geotechnics* **70** (2015) 169–177.
- [28] Tschuchnigg, F., Schweiger, H.F. and Sloan, S.W. Slope stability analysis by means of finite element limit analysis and finite element strength reduction techniques. Part II: Back analyses of a case history. *Computers and Geotechnics* **70** (2015), 178–189.
- [29] Zienkiewicz, O.C., Humpheson, C., and Lewis, R.W. Associated and non-associated visco-plasticity and plasticity in soil mechanics. *Géotechnique* **25** (1975) 671–689.